CHAPTER 5

Drivers of the short-scale spatial variability of the haploid:diploid ratio of biphasic life cycles

ABSTRACT

The haploid and diploid phases of isomorphic biphasic life cycles often occur in the environment at uneven abundances. These have been documented as a haploid-to-diploid ratio (H:D) different from 1. Furthermore, the spatial variability of the H:D has been documented within the same population related to intertidal height and degree of hydrodynamic stress. It may reflect conditional differentiation driving the niche partitioning that has been argued necessary for the prevalence of biphasic life cycles. The objective of this work was to investigate which vital rates and demographic features could be involved in conditional differentiation and efficiently generate a conspicuous H:D variability at a fine spatial resolution. A previously tested matrix demographic model was upgraded to include spatial discretization together with the required improvement in the biological resolution. Both the analytical solution to the long term stable H:D and the numerical solutions to the transient H:D were determined. Their dynamics were tested for time and space variation, degree of dissimilarity between phases and type of life strategy. The H:D spatial distribution was always smoothed relative to the ploidy fertility ratio and overrated relative to the ploidy survival ratio. Among these, ploidy dissimilar survival rates where the only able to respond to a spatially heterogeneous environment efficiently creating a niche partition. However, it was found that ploidy dissimilar spore dispersal could also create the necessary niche partition without the need for conditional differentiation of the ramets.

Keywords: Biphasic, demographic matrix, G:T, H:D, isomorphic, life cycle, spatial variation, transient trajectory.

INTRODUCTION

Algae species with isomorphic biphasic life cycles have their alternating haploid and diploid generations cohabiting. The ratio between the field abundances of these opposite ploidy phases (H:D) has long been an intriguing subject. It would be expected to find even abundances between ploidy phases as a consequence of isomorphicity. However, these often are uneven as reported by Santos and Nyman (1998), Engel et al (2001), Mudge and Scrosati (2003), Thornber and Gaines (2003), Scrosati and Mudge (2004a and b) and Dyck and deWreede (2006), among many others. The persistency of uneven ploidy phase abundances may be taken as evidence about partition of niches. Hughes and Otto (1999) have proved the necessity for a niche partition in order for one of the ploidy phases not to exclude the other, eliminating the biphasic life cycle and fixing it as a monophasic one. In their adimensional model solved for steady state, the niche partition was due to conditional differentiation of the ploidy phases and led to a fixed H:D. The consequences of conditional differentiation on either a space or time variability of the H:D were accessed in posterior works by other authors. About the time variability, the forth chapter demonstrated that, even in steady environments, the differential adaptation of ploidy phases produced a time variation of the H:D which was set by the own biphasic life cycle structure. About the space variability, the third chapter has demonstrated that the large geographical variation of the H:D observed for certain species (Thornber and Gaines 2003) could be easily generated by differential survival rates between ploidy phases in species with survival dominated life strategies, whereas it hardly could be generated by differential fertility rates. But the spatial variability of the H:D does not occur only at a large geographical scale between populations clearly set apart and subject to diverging environments. It has also been documented within the same population related to intertidal height, degree of hydrodynamic stress and distance from shore (Destombe et al 1989, Lindgren et al 1998, Engel et al 2001, Mudge and Scrosati 2003, Scrosati and Mudge 2004b, and Dyck and deWreede 2006). It was the objective of this work to investigate which vital rates and demographic features could be involved in conditional differentiation and efficiently generate a conspicuous H:D variability at a fine spatial resolution. The H:D spatial pattern was both accessed for the stable population structure and for the transient period prior to stabilization. In the end, the current work tried to relate the results obtained with the H:D short-scale spatial variation reported in the works mentioned above.

METHODS

A provisional spatially adimensional demographic model of an isomorphic biphasic life-cycle was developed. This model was adapted to include spatial discretization over a horizontal plan. It implied upgrading the biological resolution of the model to include detail in the mechanisms of spore dispersal. It was determined both the analytical solution to the long term stable population structure and the numerical solutions to the transient phase. Their dynamics were tested for time and space variation, dissimilar life cycle traits, degree of dissimilarity between phases and type of life strategy, i.e. population dynamics dominated by fertility, growth or looping (see below).

The spatially adimensional biphasic life-cycle model was similar to the ones in the preceding chapters, where each phase has one spore stage and three ramet size classes. The transitions between stages were classified as fertility type vital rates ('F' for fecundity and spore survival), growth type vital rates ('G' for growth) and looping type vital rates ('L' for stasis, breakage and clonal growth). A demographic matrix was constructed (equation 1) where the survival of the carpospores (S_{carp}) and of the tetraspores (S_{tet}) was kept constant; the haploid and diploid fecundities were dependent on the parameters f_H and f_D and a size class weight factor (wf_j, j is the column index) was introduced to account for different fecundities of each size class. The haploid and diploid growth rates were dependent on the parameters g_H and g_D; and the haploid and diploid looping rates were dependent on the parameters l_H and l_D. The looping rates were split in the demographic matrix so that their column sums were always l_H or l_D. The projection interval (Δt) was one month.

$$\left[\begin{array}{cccc:cccc} 0 & 0 & 0 & 0 & 0 & f_D.wf_j & f_D.wf_j & f_D.wf_j \\ S_{tet} & l_H & l_H/4 & l_H/8 & 0 & 0 & 0 & 0 \\ 0 & g_H & 3l_H/4 & l_H/8 & 0 & 0 & 0 & 0 \\ 0 & 0 & g_H & 6l_H/8 & 0 & 0 & 0 & 0 \\ \hdashline 0 & f_H.wf_j & f_H.wf_j & f_H.wf_j & 0 & 0 & 0 & 0 \\ 0 & 0 & 0 & 0 & S_{carp} & l_D & l_D/4 & l_D/8 \\ 0 & 0 & 0 & 0 & 0 & g_D & 3l_D/4 & l_D/8 \\ 0 & 0 & 0 & 0 & 0 & 0 & g_D & 6l_D/8 \end{array}\right] \times \left[\begin{array}{c} 'Tet.' \\ '1' \\ '2' \\ '3' \\ \hdashline 'Carp.' \\ '4' \\ '5' \\ '6' \end{array}\right] \qquad \text{(eqn.1)}$$

Spatial discretization was inserted assuming a population scattered over a grid defined by two orthogonal axes. The x dimension is evaluated from point ‘a’ to ‘b’ at intervals of Δx and thus with $1+(b-a)/\Delta x$ points. The y dimension is evaluated from point ‘c’ to ‘d’ at intervals of Δy and thus with $1+(d-c)/\Delta y$ points. A demographic matrix was estimated for each point with its specific ploidy dissimilarities for the F, G and L parameters. These dissimilarities were tested according to two different hypotheses:

1. For each type of parameters (F, G or L) at the time there was a dissimilarity linear gradient that benefited the haploid vital rates in ‘a’ and ‘c’ and the diploid vital rates in ‘b’ and ‘d’. This scenario may represent a cross shore gradient of intertidal height and an along shore gradient of wave exposure or fresh water influence, as it has been described for isomorphic biphasic life cycle population by Destombe et al (1989), Engel et al (2001), Mudge and Scrosati (2003), Scrosati and Mudge (2004b), Dyck and deWreede (2006) and Prathep (2009). The levels of ploidy dissimilarity, named ‘disx’ for the x dimension and ‘disy’ for the y dimension, were defined as the surplus in the parameter of one phase relative to the opposite phase. Therefore, for any point (x,y), the parameters had their values estimated for the haploids and diploids as in Table I.

Table I – estimation of the parameters p_H and p_D in point (x,y) according to dissimilarity levels disx and disy.

Phase:	parameter p at point (x,y):	
	linear gradient model (hypothesis 1)	*random model (hypothesis 2)*
H	$\left[1+disx.\left(\frac{b-x}{b-a}\right)\right].\left[1+disy.\left(\frac{d-y}{d-c}\right)\right].p$	$p.(1+disx.disy.rand(-1,1))$
D	$\left[1+disx.\left(\frac{x-a}{b-a}\right)\right].\left[1+disy.\left(\frac{y-c}{d-c}\right)\right].p$	p

2. The ploidy phase dissimilarities in the F, G and L parameters were randomly distributed over the (x,y) grid (Fig.1 right). For any point (x,y) in the grid the haploid and diploid parameters were estimated as in table I. The maximum surplus was given by disx*disy. This scenario simulates, for example, a rocky intertidal area with rock pools at different elevations where the environment inside the pools is different among them and from the environment outside. This situation was documented for the isomorphic biphasic life cycle species *Gracilaria verrucosa* (Destombe et al 1989).

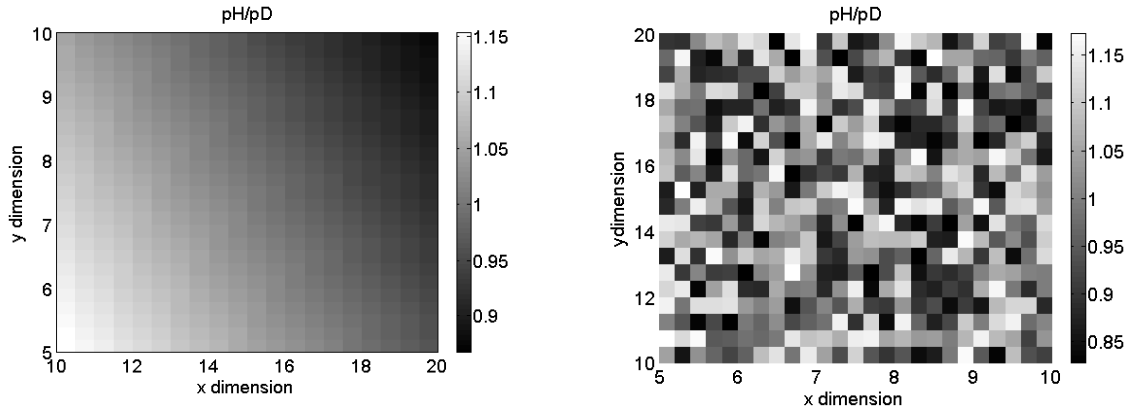

Figure 1 – spatial distribution of phase dominance in parameter p. (left) given by the linear gradient model with a=5, b=10, dx=0.2, c=10, d=20, dy=0.5, p=0.35, disx=0.05 and disy=0.1. (right) given by the random distribution model. a=5, b=10, dx=0.2, c=10, d=20, dy=0.5, p=0.35, disx=0.25 and disy=0.25.

At this stage the model was unable to simulate connectivity among the points in the grid. This was established assuming connectivity only occurred through the spores as these dispersed by diffusion. Advective transport was neglected for the sake of simplicity. It was assumed that the time interval spores may spend suspended in the water column (Δt^*) was less than one time interval of the model (i.e. one month, ($\Delta t^* < \Delta t$). Hence, after one time step every carpospore and tetraspore produced either settled, died or exited the grid. It was further assumed that, within the projection interval of one month, spores had a maximum diffusive radius (dr) corresponding to the maximum distance they could travel away from their release point during Δt^*. The spores were assumed to be randomly spread within the circumference defined by the release point and diffusive radius. At this stage the biological resolution of the life cycle was increased: during one time step the spores were released to the water column, dispersed, subject to a survival rate (sw) and finally settled. At the end of the projection interval the surviving spores made the transition to the spore stage:

$$spores_{t+1} = sw.f\sum_{j} wf_{(j)}.size\ class_{(j,t)} \qquad \text{(eqn.2)}$$

Each point (x,y) of the spatial domain had an equal probability to receive the spores produced anywhere within its diffusive radius. This was only because advective

transportation had been neglected and diffusion spread the spores randomly. Thus, the probability of one spore released from point (x_0,y_0) to arrive at point (x_p,y_p) was the exact same probability of one spore released from point (x_p,y_p) to do the inverse path, which could be approximated by $\Delta x\Delta y/(\pi dr^2)$. Hence the spores at point (x_0,y_0) and time t+1 could be estimated by equation 3. For the discrete model implementation the integral was estimated numerically as Riemann's integral.

$$sw.\int_{x_0-dr}^{x_0+dr}\int_{y_0-\sqrt{dr^2-(x-x_0)^2}}^{y_0+\sqrt{dr^2-(x-x_0)^2}} f_{(x,y)}\sum_j size\ \ class_{(j,x,y,t)}.wf_{(j)}\,dy.dx.\frac{\Delta x.\Delta y}{\pi.dr^2} \qquad \text{(eqn.3)}$$

In the following time interval the settled spores germinated and grew to the first size class subjected to a survival rate (ss):

$$1^{st}\ size\ class_{(x,y,t+1)} = spore_{(x,y,t)}.ss + \ldots \qquad \text{(eqn.4)}$$

The simulation of spore dispersal was incorporated into the demographic model by splitting the demographic matrix into its transition and fertility components. This was done in a slightly different way from what is usualy done in Markov chain analysis. The demographic model (equation 5) became $N_{t+1}=T*N_t+Fv_t$ where T is the (8,8) matrix of transitions of individuals older than one projection interval (G and L) and Fv is the (8,1) vector of spore production and dispersal (F). To estimate Fv the equations 2,3 and 4 where applied differentially to haploids and diploids. So, besides its own f, each ploidy phase also had its own dr, sw and ss.

$$N_{t+1}=\left[\begin{array}{cccc|cccc} 0 & 0 & 0 & 0 & 0 & 0 & 0 & 0 \\ ss_{tet} & l_G & l_G/4 & l_G/8 & 0 & 0 & 0 & 0 \\ 0 & g_G & 3l_G/4 & l_G/8 & 0 & 0 & 0 & 0 \\ 0 & 0 & g_G & 6l_G/8 & 0 & 0 & 0 & 0 \\ \hline 0 & 0 & 0 & 0 & 0 & 0 & 0 & 0 \\ 0 & 0 & 0 & 0 & ss_{carp} & l_T & l_T/4 & l_T/8 \\ 0 & 0 & 0 & 0 & 0 & g_T & 3l_T/4 & l_T/8 \\ 0 & 0 & 0 & 0 & 0 & 0 & g_T & l_T/8 \end{array}\right]\times N_t+\left[\begin{array}{c} spores_{(x_0,y_0,t+1)} \\ 0 \\ 0 \\ 0 \\ spores_{(x_0,y_0,t+1)} \\ 0 \\ 0 \\ 0 \end{array}\right] \qquad \text{(eqn.5)}$$

The demographic model was tested for a wide range of f, g and l parameter values. The g and l ranged from 0 to 1 constrained to the fact that survival (the column sum of g and l) could not exceed 1. The product sw*ss was tested ranging from 1 to 10^{-6}. It was only accepted the combinations of parameters that gave an asymptotic population growth between 1 and 1.11.

When the diffusive radius was set smaller than both Δx and Δy there was no dispersal. The demographic model in equation 5 corresponded to the simplified form in equation 1 with the differences that f_P corresponds to $sw_P * f_P$ and S_P to ss_P (here P stands for ploidy, H or D). The no-dispersal hypothesis was the control against which the alternative hypothesis of dispersal was tested. Furthermore, using equation 1 it was possible to use matrix algebra theorems to analytically estimate the asymptotic population growth rate (λ) and its elasticities to the F, G and L model parameters (Caswell 2001). Under the hypothesis of dispersal the demographic model in equation 5 could not be simplified. However, it was observed that this model also always tended asymptotically to a stable population structure and growth rate and was ergodic, i.e: independent of the initial conditions, with a constant growth rate both over time and space, and where the proportions of the stages were fixed both intra and inter spatial points. This was analytically demonstrable: the spatially explicit population model could be written as one single demographic matrix, irreducible and primitive according to the Perron-Frobenius theorem. This type of matrices always has a dominant eigenvalue which sets the asymptotic growth rate and an associated eigenvector which sets the asymptotic population structure (Caswell 2001).

From the paragraph above it was always possible to estimate the elasticities of λ to the F, G and L model parameters. It allowed classifying the life strategy resulting from each particular combination of parameters as dominated by F, G or L. This is a life strategy where the bulk of the elasticities of λ are to the F, G or L entries in the demographic matrix. It is simple and direct as the elasticities of λ to the entries in the demographic matrix always add up to 1. This type of classification was introduced in plant demography by Franco and Silverthorne (1996) and Oostermeijer et al (1996). It was later applied to the demography of isomorphic biphasic life cycles in the preceding chapters of the current thesis, which tested demographic matrices similar to that of equation 1. The best combinations of parameters to yield the F, G and L dominated life strategies were thus known *a priori*.

With no spore dispersal

In the absence of dispersal, the algorithms of the above formulated dissimilarity hypotheses were the only cause for the ramet abundance differences between points. The ramet abundance variability depended on the type of life strategy: i) in fertility dominated life strategies the total abundance of ramets was positively correlated with the total fertility, i.e. with f_G*f_T; ii) in looping dominated life strategies, the ramet abundance correlated with the maximum looping rates, either l_G or l_T; iii) in growth dominated life strategies, the ramet abundance was a function of both g_G*g_T and the maximum between g_G and g_T.

In the absence of dispersal, The H:D followed the patterns set by the linear gradient model (Fig.1 left) and the random model (Fig.1 right), being dependent on its sensitivity to the f, g and l ratios between phases (Fig.2 a, b and c). The slopes in this figure show the sensitivity of the H:D to the ratio between ploidy dissimilar vital rates. It was bigger in l than f or g. In the case of f_H:f_D the slope was negative (Fig.2a) because through fertility each phase contributed to the other. So, the H:D spatial pattern was reversed from the f_H:f_D spatial pattern. In the case of g_H:g_D the slope was negative for the spores and smaller ramets while positive for the bigger ramets (Fig.2b). So, the H:D spatial pattern was reversed from the g_H:g_D spatial pattern when estimated only within the first size class whereas it was equal to the g_H:g_D spatial pattern when estimated only within the second or third size classes. In the case of l_H:l_D the slope was always positive (Fig.2c). So, the H:D spatial pattern was always equal to the l_H:l_D spatial pattern.

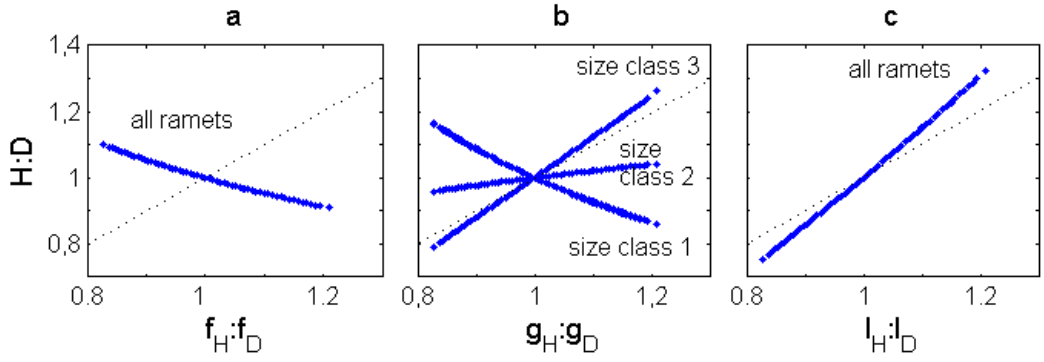

Figure 2 – The H:D under no dispersal in simulations of (A) fertility dominated, (B) growth dominated and (C) looping dominated demographic models. x axis: the respective vital rates ratio in each point. y axis: the assymptotic H:D in each point.

With spore dispersal

When spore dispersal was implemented, and thus also connectivity, it was numerically verified that the population still always converged asymptotically to an ergodic stable structure and growth rate. Therefore, for any point (x_0,y_0) inside the grid it was possible to determine a semi-analytical solution the stable population structure (equation 6) which provided tools that proved helpful for the analysis. Its deduction is available in Appendix VI.

$$N_{(x_0,y_0,t_s)} = \lim_{t\to+\infty} \frac{N_{(x_0,y_0,t+t_s)}}{\lambda^t} = \lambda^{-1}.inv\left(I - T_{(x_0,y_0)}.\lambda^{-1}\right)Fv_{(x_0,y_0,t_s)} \quad \text{(eqn.6)}$$

where t_s is a specified time were the whole population is already at steady state, λ is the assimptothic growth rate, both the Fv vector and the population vector (N) are standardized to the population size at time t_s and I is the identity matrix. Equation 6 has affinity with the Lotka's integral equation for the instantaneous growth rate r, Volterra's integral equations and the McKendrick-von Förster models. The maternity or birth functions integrate the Fv vector and include immigrant spores. The equation 6 was tested for the life strategies, being found that:

$$\lim_{\lambda\to f(T)} \frac{N_{(x_0,y_0,t+t_s)}}{\lambda^t} = T^*_{\max}.Fv_{\min}.\lambda^{-1}$$

$$T^*_{\max} = .inv\left(I - T_{(x_0,y_0)}.\lambda^{-1}\right) = \left[\begin{array}{c|c} \max & 0 \\ \hline 0 & \max \end{array}\right] \quad \text{(eqn.7)}$$

$$Fv_{\min} = [\min \quad 0 \quad 0 \quad 0 \quad \min \quad 0 \quad 0 \quad 0]$$

$$\lim_{\lambda\to f(F)} \frac{N_{(x_0,y_0,t+t_s)}}{\lambda^t} = T^*_{\min}.Fv_{\max\,(x_0,y_0,t_s)}.\lambda$$

In the T* matrix each of the four blocks is either relative to intra-ploidy transitions (maximum or minimum) or inter-ploidy transitions (0). The λ was the global population growth rate whereas Fv was dependent on the reproductive out-put of the entire population. This analysis showed that whenever a population was globally dominated by one type of transitions, so was the population structure at any point. As λ tended to be mainly given by the fate of the ramets (lim[λ→f(T)]) the asymptotic population

structure at any point ($N(x_0,y_0,t+t_s)/ \lambda^t$) tended to be given by the fate of the ramets ($T^*_{max}.Fv_{min}$) and the dissimilarities between the matrix T ploidy blocks. Notice matrix T has both G and L vital rates. On the other hand, as λ tended to be mainly given by the production of offspring ($\lim[\lambda \rightarrow f(F)]$) the asymptotic population structure at any point tended to be given by the production of offspring ($T^*_{min}.Fv_{max}$) and the ploidy dissimilarities between its Fv entries. Furthermore, as the connectivity between the distinct points of the population was set by the Fv vector, the more the life strategy was dominated by survival (T) the less it was influenced by connectivity.

Spore dispersal was set increasing the diffusive radius to a value bigger than both Δx and Δy. The H:D dynamics was generally similar to its dynamics without spore dispersal, yet even more evident. This is shown in figure 3 for simulations of F, G and L dominated life strategies with ploidy dissimilarities imposed over the respective f, g and l parameters by the random dissimilarity hypothesis and subject to dispersal or no dispersal. The spore dispersal had two effects. One was setting connectivity between points, which smoothed the dissimilarities in the F vector all along the grid. Hence, if ploidy dissimilarities were imposed in F the H:D spatial variability was also smoothed (Fig.3F). The other effect was spore loss through the grid borders, decreasing the overall fertility and the population growth rate while increasing the sensitivity of the population to the fate of the ramets (G and L in matrix T). So, when ploidy dissimilarities were imposed over matrix T, in G or L dominated life strategies, the effect of spore loss overtook the effect of connectivity to enhance the H:D spatial variability (Figures 3, G and L). This was particularly evident when of dissimilarities imposed over L rates in L dominated life-strategies.

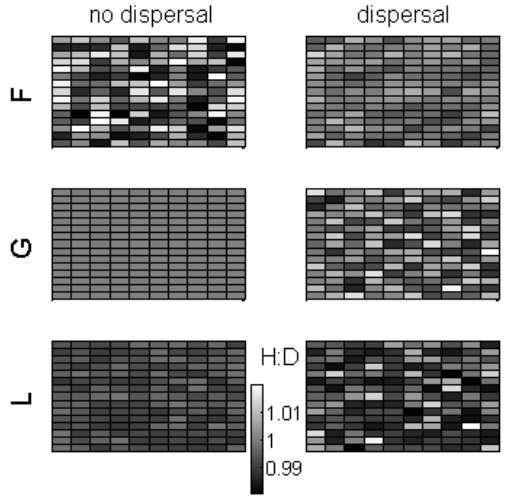

Figure 3 – Stable H:D distribution simulated by the random dissimilarity model. disx.disy=0.04. F: fertility dominated life strategy with dissimilarities imposed over f. G: growth dominated life strategy with dissimilarities imposed over g. L: looping dominated life strategy with dissimilarities imposed over l. No dispersal: $dr_{tet}=dr_{carp}=0.5$. Dispersal: $dr_{tet}=dr_{carp}=2$.

As spores were lost through the edges of the population, the supply of recruits was weaker there. Therefore, the points closer to the centre were more abundant in all stages (Fig.4) despite the asymptotic growth rate being constant all over the domain. It was like a lump with the abundance in the z axis constantly magnified over time. This spatial distribution of the abundances caused a non-linearity in the spatial distribution of the H:D. The dependency of the F vector in point (x_i,y_i) from the information in point (x_j,y_j) was given by the ratio of the abundances between those two points (a_j/a_i). This was a measure of the relative information flow standardized to the information self-loop equaling 1 (a_i/a_i). So, it could be seen from figure 4 that the information flow was concentrical. This circular pattern imposed over an orthogonal grid got the points in the corners less connected than the points in the edges and thus more dependent on their inner demographic conditions. When these were of ploidy dissimilarities in the T matrix the H:D was particularly hyped in the corners (fig.5).

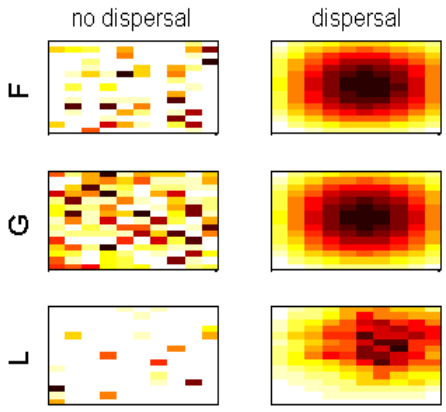

Figure 4 – Stable abundance distributions simulated by the random dissimilarity model. The same simulations as in figure 3 but the colour scale is the abundance rather than the H:D. Darker is more abundant. disx.disy=0.04. F: f dominated life strategy with dissimilarities imposed over f. G: g dominated life strategy with dissimilarities imposed over g. L: l dominated life strategy with dissimilarities imposed over l. No dispersal: $dr_{tet}=dr_{carp}=0.5$. dispersal: $dr_{tet}=dr_{carp}=2$.

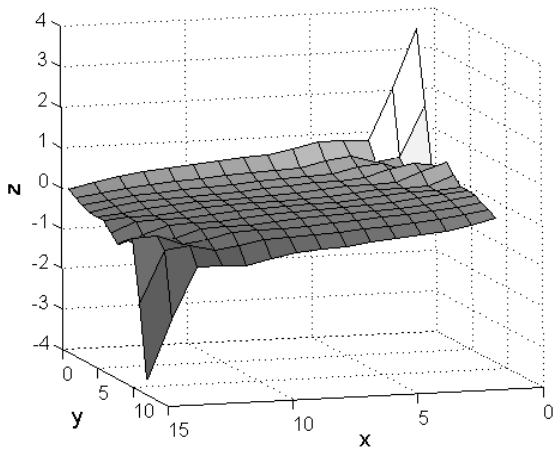

Figure 5 – H:D differential between dispersal ($dr_{tet}=dr_{carp}=2$) and no dispersal ($dr_{tet}=dr_{carp}=0.2$) in an L dominated life strategy with dissimilarities imposed over L by the linear gradient model.
Z axis: $\log(H:D_{dispersal})-\log(H:D_{control})$. disx=0.5, disy=0.05. f=5, g=0.1, l=0.8, $ss_{carp}=ss_{tet}=10^{-2.5}$, $sw_{carp}=sw_{tet}=10^{-2.5}$ and wf=[0 10 500 1000 0 10 500 1000].

When the reproductive out-put was large the ramets growth rates contributed significantly to the opposite phase as it was shown in fig.2. When ploidy dissimilarities were imposed over the growth rates, in the absence of dispersal, the H:D spatial pattern was: (i) reversed from the g_H:g_D in the smaller ramets, (ii) like the g_H:g_D but smoothed for the medium ramets and (iii) like the g_H:g_D but overrated for the large ramets. The result was the H:D over all ramet size classes was non-linear with respect to space. When spore dispersal was set the heterogenic effects of connectivity and spore loss were added, which could easily result in an even more awkward H:D spatial pattern (fig.6) that totally miss-fitted the fitness ratio given by the g_H:g_D (fig.1 left).

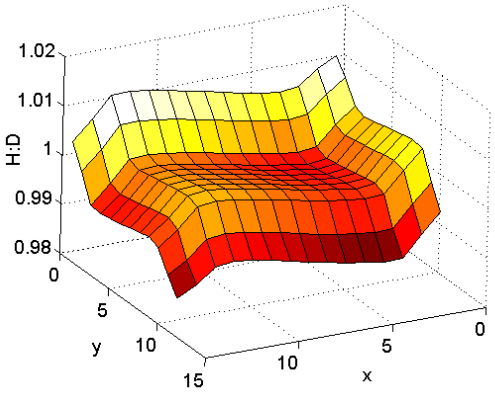

Figure 6 – Awkward effect in the H:D spatial distribution of ploidy dissimilarities in g according to the linear gradient model. Colour scale: H:D. disx=0.2, disy=0.2, dr_{tet}=dr_{carp}=3, sw_{tet}=sw_{carp}=$10^{-1.5}$, ss_{tet}=ss_{carp}=10^{-2}, f=5, wf=[0 10 500 1000 0 10 500 1000], g=0.5 and l=0.1.

Increasing the size of the diffusive radius (relatively to the size of the domain) had a stronger effect in spore loss than in connectivity and thus resulted in a lower population growth rate, a higher sensitivity to the matrix T* and a population structure bias towards the bigger ramets. Thus, increasing spore dispersal caused the H:D to asymptotically converge towards the one set by the T* matrices. This convergence was quicker in the edges of the grid than in the centre.

Ploidy dissimilar spore dispersal

Testing for ploidy phase dissimilarities in spore dispersal showed the phase with smaller dr had the bell shape abundance distribution (like the one of fig.4) more pronounced. Hence, it dominated in the centre and was dominated in the edges (similar to fig.7, F and G). This pattern was more pronounced the bigger the ploidy differences in the diffusive radius and was independent of the type of life strategy. When dissimilarities in

f, g or l were added, the H:D asymptotic distribution was the linear combination of the distribution imposed by the dissimilarities in f, g or l with the distribution imposed by the dissimilarities in dr (fig.7). However, the linear combinations were not equally weighted. For the simulations over L the effect of the ploidy dissimilarities in l largely overcame the effect of the ploidy dissimilarities in dr. Nevertheless, for the L simulation in figure 7 disx and disy were half of what they were in the F and G simulations while the maximum differential between l_g and l_t was one tenth of the differential between dr_{carp} and dr_{tet}.

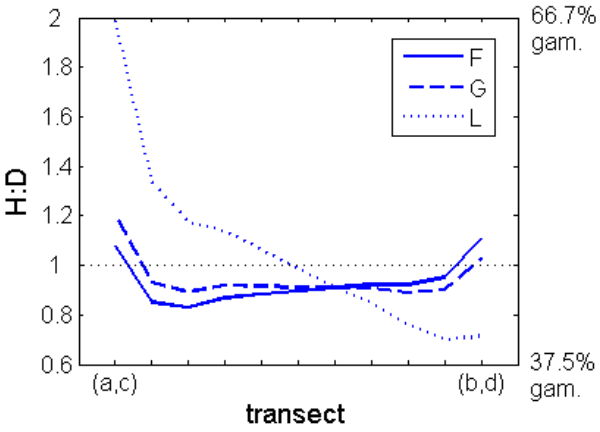

Figure 7 – stable H:D along a transect from (a,c) to (b,d). Simulations in the F, G and L domains with ploidy dissimilarities in the respective vital rates and in dr. Gametophytes (gam) are the haploids.

Transient dynamics

Following colonization, in the absence of spore dispersal where formed patches of ploidy dominance matching the used dissimilarity hypothesis (the linear gradient was used in this example). In fertility dominated life strategies with ploidy dissimilarities over fertility rates (from now on called “F simulations”) these patches wobbled back and forth until settlement in the stable H:D (animation 1A), and the same for growth dominated life strategies with ploidy dissimilarities over growth rates (from now on called “G simulations”). During this latter the patches suffered conspicuous changes in ploidy dominance (animation 2A). In looping dominated life strategies with ploidy dissimilarities over looping rates (from now on called “L simulations”) the patches tended slowly and monotonically to the stable H:D (animation 3A). Introducing spore dispersal smoothed the transient phase in F simulations (animation 1B), enhanced it in L simulations (animation 3B) and turned it into something very awkward in G simulations (animation 2B) as a consequence of the processes debated in the second-last paragraph

of section 3.2. Given ploidy dissimilarities exclusively in the diffusive radius, in the centre of F and G simulations was constantly favored the phase with the smaller dr whereas the edges was the other way around (animations 1C and 2C). It showed the contrast between the dependencies of locally *vs* non-locally produced recruits. In L simulations where formed patches dominated by the first ploidy to arrive at the spot and tending slowly and monotonically to the asymptotically stable H:D (animation 3C). The ploidy dissimilarities in spore dispersal conjugated evenly with the ploidy dissimilarities in fertility rates (animation 1D). Furthermore, the oscillations increased amplitude and duration, revealing an interaction between both. Ploidy dissimilar growth rates where overwhelmed by ploidy dissimilar spore dispersal (animation 2D). Ploidy dissimilar looping rates largely overcame ploidy dissimilar spore dispersal on the long run (animation 3D). In the L simulations was also evident an interaction between both types of ploidy dissimilarities.

Animation 1 – H:D transient trajectory for a population with a fertility dominated life strategy. The colour scale is log(H:D) and it changes bounds for t>13. (A) with ploidy dissimilarities in the fertility rates according to the linear gradient hypothesis and without spore dispersal. $dr_{carp}=dr_{tet}=0.5$, disx=disy=0.5, f=7 and colonization at $N_{i,j,0}$=[1 0 0 0 1 0 0 0]. (B) with ploidy dissimilarities in the fertility rates according to the linear gradient hypothesis and with spore dispersal. $dr_{carp}=dr_{tet}=5$, disx=disy=0.5, f=10 and colonization at $N_{i,j,0}$=[1 0 0 0 1 0 0 0]; (C) with ploidy dissimilarities in spore dispersal. $dr_{carp}=3$, $dr_{tet}=6$, disx=disy=0, f=14 and colonization at $N_{10,8,0}$=[1 0 0 0 1 0 0 0]; (D) with ploidy dissimilarities in the fertility rates according to the linear gradient hypothesis and in the spore dispersal. $dr_{carp}=3$, $dr_{tet}=6$ and disx=disy=0.5, f=10 and colonization at $N_{10,8,0}$=[1 0 0 0 1 0 0 0]; (all) $ss_{tet}=ss_{carp}=10^{-1.8}$, $sw_{tet}=sw_{carp}=10^{-1.2}$, g=0.12, l=0.05, wf=[0 10 500 1000 0 10 500 1000], a=1, b=15, $\Delta x=\Delta y=1$, c=1 and d=15.

Animation 2 – H:D transient trajectory for a population with a growth dominated life strategy. The colour scale is log(H:D) and it changes bounds for t>20 and t>40. (A) with ploidy dissimilarities in the growth rates according to the linear gradient hypothesis and without spore dispersal. $dr_{carp}=dr_{tet}=0.5$, disx=disy=0.2, f=3, and colonization at $N_{i,j,0}$=[1 0 0 0 1 0 0 0]. (B) with ploidy dissimilarities in the growth rates according to the linear gradient hypothesis and with spore dispersal. $dr_{carp}=dr_{tet}=3$, disx=disy=0.2, f=7 and colonization at $N_{i,j,0}$=[1 0 0 0 1 0 0 0]; (C) with ploidy dissimilarities in spore dispersal. $dr_{carp}=3$, $dr_{tet}=6$, disx=disy=0, f=5 and colonization at $N_{10,8,0}$=[1 0 0 0 1 0 0 0]; (D) with ploidy dissimilarities in the looping rates according to the linear gradient hypothesis and in the spore dispersal. $dr_{carp}=3$, $dr_{tet}=6$,

disx=disy=0.5, f=5 and colonization at $N_{10,8,0}$=[1 0 0 0 1 0 0 0]; (all) $ss_{tet}=ss_{carp}=10^{-2}$, $sw_{tet}=sw_{carp}=10^{-1.5}$, g=0.55, l=0.05, wf=[0 10 500 1000 0 10 500 1000], a=1, b=15, $\Delta x=\Delta y=1$, c=1 and d=15

Animation 3 – H:D transient trajectory for a population with a looping dominated life strategy. The colour scale is log(H:D) and it changes bounds for t>20 and t>50. (A) with ploidy dissimilarities in the looping rates according to the linear gradient hypothesis and without spore dispersal. $dr_{carp}=dr_{tet}=0.5$, disx=disy=0.1, f=3, and colonization at $N_{i,j,0}$=[1 0 0 0 1 0 0 0]. (B) with ploidy dissimilarities in the looping rates according to the linear gradient hypothesis and with spore dispersal. $dr_{carp}=dr_{tet}=5$, disx=disy=0.1, f=5 and colonization at $N_{i,j,0}$=[1 0 0 0 1 0 0 0]; (C) with ploidy dissimilarities in spore dispersal. $dr_{carp}=3$, $dr_{tet}=6$, disx=disy=0, f=6 and colonization at $N_{10,8,0}$=[1 0 0 0 1 0 0 0]; (D) with ploidy dissimilarities in the looping rates according to the linear gradient hypothesis and in the spore dispersal. $dr_{carp}=3$, $dr_{tet}=6$, disx=disy=0.1, f=5 and colonization at $N_{10,8,0}$=[1 0 0 0 1 0 0 0]; (all) $ss_{tet}=ss_{carp}=10^{-1.8}$, $sw_{tet}=sw_{carp}=10^{-1.2}$, g=0.05, l=0.85, wf=[0 10 500 1000 0 10 500 1000], a=1, b=15, $\Delta x=\Delta y=1$, c=1 and d=15.

DISCUSSION

The model in the absence of spore dispersal served both as a control and a comparison to previous works. It gave results identical to the ones in chapters 2 and 4: 1) it clearly differentiated the dynamics of fertility and looping (related to survival) dominated life strategies and revealed the growth dominated life strategy as a mid-term; 2) it showed that growth contributes significantly to the abundance of the bigger ramets of the own ploidy phase but also to the abundance of the smaller ramets of the opposite ploidy phase; 3) it showed that in each life strategy domain the H:D is more responsive to the respective type of vital rates; and 4) it showed that the responsiveness of the H:D to looping vital rates in the looping dominated life strategies is much higher than to fertility or growth rates in any life strategy. The extreme responsiveness of isomorphic biphasic life cycles to ploidy dissimilarities in survival rates had already been detected by Hughes and Otto (1999) for its evolution and stability, and by Engel et al (2001) for its asymptotic population growth rate. This match between the present model and previous spatially adimensional models strengthens the confidence in the proceeding findings. The introduction of spore dispersal maintained this same global dynamics.

Furthermore, the analytical solution to the spatially explicit stable structure demonstrated that the fundamental drive (dissimilarities in fertility, growth or looping) for the H:D and its fine-scale spatial variability must be common to all locations within the population bounds.

Ploidy dissimilar fecundity rates were reported by Scrosati et al (1994), Gonzalez and Meneses (1996), Santos and Duarte (1996), Servière-Zaragoza and Scrosati (2002), Thornber and Gaines (2004) and Thornber et al (2006). However, this work has shown the H:D spatial distribution is always reversed and smoothed relative to the f_D:f_H spatial distribution. Reversed means that, at each location, the population is dominated by the phase locally less fit, i.e: with smaller fecundity rates. Smoothed means that, even if the H:D was not reversed, it would be inefficient to create a spatial niche partition by adapting the fecundity rates differentially between ploidy phases. This does not mean ploidy dissimilar fecundity rates may not exist, but only that they may not be a tool for the conditional differentiation of ploidy phases that Hughes and Otto (1999) shown necessary for the stability and evolution of biphasic life cycles. Thornber and Gaines (2004) proposed fixed ploidy dissimilar fertility rates as the cause for the global average H:D but not for its spatial variability.

Ploidy dissimilar ramet growth rates were reported by Destombe et al (1989), Gonzalez and Meneses (1996), Carmona and Santos (2006), Thornber et al (2006) and Pacheco-Ruíz et al (2011). However, this work has shown the H:D spatial distribution can easily mismatch the g_D:g_H spatial distribution. This is because the phase that grows better contributes to its own dominance over the bigger ramets through the growth path but also to the dominance of the opposite phase over the smaller ramets through the fertility path. This was already shown in chapter 2, which also argued about this dynamics being a possible tool for the stability of isomorphic biphasic life cycles. However, in the current work, when it was imposed spore dispersal and a g_D:g_H fine-scale spatial gradient related to environmental conditions, the patterns of ploidy dominance became very smooth and very strange, totally miss-fitting the H:D spatial pattern expected to optimize the overall life cycle fitness. It was even possible to find the local dominance of the phase less fit, i.e: with smaller growth rates, particularly following colonization. Therefore, the possibility of ploidy dissimilar growth rates being a tool for the conditional differentiation of ploidy phases that Hughes and Otto (1999) shown necessary for the stability and evolution of biphasic life cycles is

restricted to survival dominated life strategies and to being conjugated with ploidy dissimilar looping rates.

Ploidy dissimilar looping rates were reported by Destombe et al (1989), Gonzalez and Meneses (1996), Carmona and Santos (2006), Thornber et al (2006), Vergés et al (2008) and Pacheco-Ruíz et al (2011). This work has shown that the spatial distribution of the H:D always matches the l_H:l_D distribution and supersedes it. This is true for any location within the population, following colonization or at the asymptotic stable population structure. Therefore, ploidy dissimilar looping rates are an excellent tool for the conditional differentiation of ploidy phases that Hughes and Otto (1999) shown necessary for the stability and evolution of biphasic life cycles and the likeliest answer for the fine scale spatial variability of the H:D reported by Destombe et al (1989), Engel et al (2001), Mudge and Scrosati (2003), Scrosati and Mudge (2004b) and Dyck and deWreede (2006). It is particularly interesting the shift of phase dominance at a very short spatial scale (few meters) for populations of *Gelidium canarensis* in the stable population structure (Lindgren et al 1998). The present work suggests such shifts can hardly be caused by anything else besides ploidy dissimilar looping rates in survival dominated life cycles.

The development of the spatially explicit model unveiled the importance of spore dispersal on the H:D dynamics, summarized in four points:

1. Spore dispersal imposes connectivity between different locations within the population. It smoothes the H:D where the population is more intra-connected, which is in its centre. This smoothing effect is bigger the more spores are produced; that is in fertility dominated life strategies.

2. Spore dispersal increases mortality in the edges of the population. It makes the edges more dependent on the fate of the ramets and thus more sensitive to ploidy dissimilarities there in. Therefore, the H:D is overrated relative to what it would be if there was no spore dispersal. The non-linearity of the H:D inflation in the edges during the simulations, with more H:D inflation in the corners of the grid, reports to reality by showing that the relation between connectivity and dependency from local conditions is non-linear.

3. From points (1) and (2) it can be concluded that, given the existence of ploidy dissimilarities in the ramet rates, the spore dispersal smoothes the H:D in the centre of the population while inflates it in the edges. The more the spores disperse the smoother the H:D is in the centre and the more uneven it is in the edges.

In the current model the spore dispersal was simulated by giving it a maximum dispersive range over the projection interval of one month. With a finer temporal and biological resolution this can be traced back to the amount of time spores take to settle and their mortality rates while suspended. Spore performance has often been reported to be ploidy dissimilar (Scrosati et al 1994, Gonzalez and Meneses 1996, Destombe et al 1989, Garza-Sanchez et al 2000, Carmona and Santos 2006, Roleda et al 2008 and Pacheco-Ruíz et al 2011). The effect of ploidy dissimilar spore dispersal on an uneven H:D was reported by Pacheco-Ruíz et al (2011). The current work has further demonstrated it alone was enough to create a conspicuous spatial (patchy) niche partition between ploidy phases. In looping dominated life strategies the H:D patches showed great constancy, whereas in fertility and growth dominated life strategies the patches wobbled back and forth at a fast rate. A similar transient behaviour was simulated in chapter 4 for the adimensional case. There, it was found the H:D cyclic oscillations could be obtained from a ploidy uneven initial population structure, ploidy dissimilar fertility rates and/or ploidy dissimilar growth rates. The present work showed that the ploidy dissimilarities in the initial population structure and/or fertility rates may be forced by ploidy dissimilar spore dispersal. This finding raises the possibility that the requirement for a niche partition that Hughes and Otto (1999) found essential for the evolution and stability of biphasic life cycles may be obtained under the form of spatial and/or temporal patches of ploidy dominance simply due to the ploidy differential capacity of spores to disperse.